Bacterial iron acquisition mediated by outer membrane translocation and cleavage of a host protein

Khedidja Mosbahi[a,1], Marta Wojnowska[a,1], Amaya Albalat[b], and Daniel Walker[a,2]

[a]Institute of Infection, Immunity, and Inflammation, College of Medical, Veterinary, and Life Sciences, University of Glasgow, G12 8QQ Glasgow, United Kingdom; and [b]Faculty of Natural Sciences, University of Stirling, FK9 4LA Stirling, United Kingdom

Edited by Steven E. Lindow, University of California, Berkeley, CA, and approved May 15, 2018 (received for review January 12, 2018)

Iron is an essential micronutrient for most bacteria and is obtained from iron-chelating siderophores or directly from iron-containing host proteins. For Gram-negative bacteria, classical iron transport systems consist of an outer membrane receptor, a periplasmic binding protein, and an inner membrane ABC transporter, which work in concert to deliver iron from the cell surface to the cytoplasm. We recently showed that *Pectobacterium* spp. are able to acquire iron from ferredoxin, a small and stable 2Fe-2S iron sulfur cluster containing protein and identified the ferredoxin receptor, FusA, a TonB-dependent receptor that binds ferredoxin on the cell surface. The genetic context of *fusA* suggests an atypical iron acquisition system, lacking a periplasmic binding protein, although the mechanism through which iron is extracted from the captured ferredoxin has remained unknown. Here we show that FusC, an M16 family protease, displays a highly targeted proteolytic activity against plant ferredoxin, and that growth enhancement of *Pectobacterium* due to iron acquisition from ferredoxin is FusC-dependent. The periplasmic location of FusC indicates a mechanism in which ferredoxin is imported into the periplasm via FusA before cleavage by FusC, as confirmed by the uptake and accumulation of ferredoxin in the periplasm in a strain lacking *fusC*. The existence of homologous uptake systems in a range of pathogenic bacteria suggests that protein uptake for nutrient acquisition may be widespread in bacteria and shows that, similar to their endosymbiotic descendants mitochondria and chloroplasts, bacteria produce dedicated protein import systems.

iron | ferredoxin | M16 protease | protein translocation | outer membrane

During pathogenesis, the ability of bacteria to acquire iron and other transition metal ions becomes a critical determining factor in the outcome of infection, because hosts invariably adopt a strategy of nutritional immunity to limit metal ion availability (1, 2). To overcome this strategy, Gram-negative bacteria produce a range of iron uptake systems that capture iron-containing substrates, such as siderophores, and host proteins at the cell surface and mediate energy-dependent iron transport to the cytoplasm (3, 4). In the case of iron-chelating siderophores, a specific TonB-dependent receptor (TBDR) binds and mediates passage of the iron-chelating compound into the periplasm, where it is bound by a cognate periplasmic binding protein and delivered to an inner membrane ABC transporter (3).

TBDRs invariably consist of a 22-strand transmembrane β-barrel that is occluded by a small globular N-terminal plug domain (5). In these systems, binding of the siderophore to the TBDR triggers release of a TonB-box located at the extreme N terminus of the receptor. TonB, which forms an inner membrane energy transducing complex with ExbBD, binds the exposed TonB-box and mechanically dislocates a force labile region of the plug domain from the barrel, allowing translocation of the substrate across the outer membrane (6, 7). In *Escherichia coli*, there are a number of well-characterized iron acquisition systems consisting of an outer membrane TBDR, a periplasmic binding protein, and an inner membrane ABC transporter, including FhuABCD and FecABCDE, which target ferrichrome and ferric citrate, respectively (8–10).

Along with iron acquisition from siderophores, some bacterial species directly target host iron-containing proteins during infection. For example, pathogenic *Neisseria* species directly target the large iron-containing protein transferrin during human infection (4, 11). Iron acquisition from transferrin uses a bipartite receptor system, consisting of a TonB-dependent receptor, TbpA, and an outer membrane lipoprotein, TbpB, which work in concert to bind transferrin and liberate its iron at the cell surface. The apoprotein is then released from the cell surface, and the liberated iron is transported to the periplasm in a TonB-dependent process, where it is bound by a periplasmic binding protein and subsequently transported to the cytoplasm by an ABC transporter (4). Homologous systems for the acquisition of iron from lactoferrin and hemoglobin are also produced by pathogenic *Neisseria* species (2).

Interestingly, TonB-dependent receptors are commonly parasitized by colicin-like bacteriocins, multidomain protein antibiotics that target bacteria closely related to the producing strain, presumably because they offer a potential route for large molecules to traverse the outer membrane (12–14). For example, colicin M uses FhuA on the surface of *E. coli*, and pyocin S2 uses the *Pseudomonas aeruginosa* ferripyoverdine receptor FvpAI (15–17). In the case of pyocin S2, mimicry of the interactions with the receptor by the natural substrate ferripyoverdine enables the pyocin to directly translocate through the lumen of FvpAI in an unfolded state. This process is TonB-dependent, with the pyocin possessing a TonB-box within an intrinsically disordered N-terminal region (18). However, although bacteriocins can parasitize transporters by mimicking the interactions of chemically and structurally dissimilar natural substrates, such as siderophores, dedicated receptor-mediated uptake systems in which the intended physiological substrate is a protein have not been previously described in Gram-negative bacteria.

We have previously shown that plant pathogenic *Pectobacterium carotovorum* and *Pectobacterium atrosepticum* are able to obtain iron from the small [2Fe-2S] iron-sulfur cluster containing

Significance

The outer membrane of Gram-negative bacteria is a highly impermeable barrier to a range of toxic chemicals and is responsible for the resistance of these bacteria to important classes of antibiotics. In this work, we show that plant pathogenic *Pectobacterium* spp. acquire iron from the small, stable, and abundant iron-containing plant protein ferredoxin by transporting ferredoxin across the outer membrane for intracellular processing by a highly specific protease, which induces iron release. The presence of homologous uptake and processing proteins in a range of important animal and plant pathogens suggests an exploitable route through which large molecules can penetrate the outer membrane of Gram-negative bacteria.

Author contributions: K.M., M.W., and D.W. designed research; K.M., M.W., and A.A. performed research; K.M., M.W., and D.W. analyzed data; and D.W. wrote the paper.

The authors declare no conflict of interest.

This article is a PNAS Direct Submission.

[1]K.M. and M.W. contributed equally to this work.

[2]To whom correspondence should be addressed. Email: Daniel.Walker@glasgow.ac.uk.

This article contains supporting information online at www.pnas.org/lookup/suppl/doi:10.1073/pnas.1800672115/-/DCSupplemental.

Published online June 11, 2018.

plant ferredoxins that are highly abundant in plants (19, 20). Interestingly, some strains of *Pectobacterium* spp. produce ferredoxin-containing bacteriocins that contain an N terminal [2Fe-2S]-containing ferredoxin domain linked to a lipid II-cleaving cytotoxic domain (19, 21). These bacteriocins specifically target other strains of *P. carotovorum* and *P. atrosepticum* and share a common TBDR receptor with plant ferredoxin, FusA, which we have recently identified and structurally characterized (22). The genetic context of *fusA* revealed an operon encoding a putative iron uptake system with additional genes encoding a TonB homolog (*fusB*), an M16 protease (*fusC*), and an ABC transporter (*fusD*), indicating an atypical iron uptake system that lacks a classical periplasmic binding protein but, unusually, contains a predicted protease (22). M16 proteases have a clamshell-like structure that can exist in open or closed conformations, with the active site located in the interior of the clamshell (23). Consequently, substrate specificity is based in part on the steric exclusion of large substrates from the active site, and substrates of M16 proteases consist largely of peptides of 30–70 residues or signal peptides from larger proteins, as in the case of the mitochondrial processing peptidase (24, 25).

In this work, we show that FusC is a periplasmically located M16 protease with a highly targeted activity against plant ferredoxin. Cleavage of ferredoxin occurs at two specific peptide bonds on the ferredoxin surface, resulting in iron release from the normally stable [2Fe-2S] ferredoxin iron sulfur cluster. Deletion of *fusC* in *P. carotovorum* results in an inability to acquire iron from plant ferredoxin, demonstrating that the Fus system is an atypical iron acquisition system. The periplasmic location of FusC shows that, in contrast to other iron acquisition systems that target host proteins, the small iron-containing ferredoxin is first transported into the periplasm before cleavage and iron release, a hypothesis supported by the accumulation of exogenous ferredoxin in the periplasm of cells lacking FusC. These data demonstrate that bacteria do in fact possess dedicated protein uptake systems, with the existence of homologous protease-containing iron acquisition systems in other Gram-negative bacteria, suggesting that the existence of bacterial protein uptake systems may be widespread.

Results

FusC Is a Metal-Dependent Protease That Selectively Targets a Plant Ferredoxin. Since FusC is a predicted metal-dependent M16 protease and is genetically linked to *fusA*, which is the outer membrane receptor for ferredoxin-containing bacteriocins and plant ferredoxin, we reasoned that a likely role of FusC is in iron acquisition, specifically to cleave plant ferredoxin to release iron from its normally stable iron sulfur cluster. Structural and functional studies of M16 proteases show that these proteins form a clamshell-like structure with the active site, which contains bound Zn^{2+} located in the interior of this structure. Zinc is bound at the HXXEH zinc-binding motif, known as the inverzincin motif, which is inverted relative to the classical HEXXH zinc-binding motif (26). To test this hypothesis, we purified His_6-tagged FusC and incubated it with His_6-tagged *Arabidopsis* ferredoxin (Fer_{Ara}) at room temperature for 60 min in the presence and absence of the metal chelator EDTA and monitored proteolytic activity by SDS-PAGE. Under these conditions, we observed degradation of Fer_{Ara} in the absence of, but not in the presence of, EDTA, indicating that FusC is a metal-dependent protease and that Fer_{Ara} is a FusC substrate (Fig. 1*A*).

Due to steric restrictions, the substrates of M16 proteases are generally limited to relatively small peptides, folded subdomains, and the unstructured regions of larger polypeptides that can access the active site (23, 24). To determine if FusC has a general proteolytic activity against other globular proteins or unfolded proteins of a similar molecular weight to ferredoxin (10 kDa), FusC was incubated with the small and stable colicin immunity proteins Im3 and Im6 (9 kDa), the RNase domain of colicin E3, E3 RNase (12 kDa), and its well-characterized intrinsically unfolded variant E3 RNase Y64A (12 kDa) (27, 28). Cleavage was not observed in any cases, indicating that FusC is a highly specific protease (*SI Appendix*, Fig. S1).

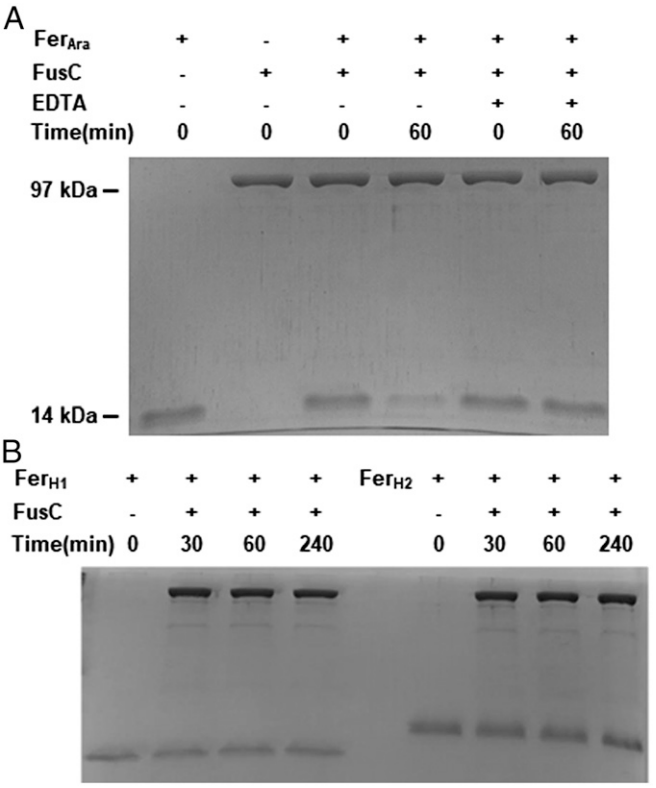

Fig. 1. FusC specifically cleaves plant ferredoxin. Purified His-tagged FusC (1 μM) was incubated in the presence or absence of either plant ferredoxin Fer_{Ara} (*A*) or human ferredoxin Fer_{H1} or Fer_{H2} (*B*) (10 μM) at room temperature in 50 mM Tris·HCl and 50 mM NaCl, pH 7.5. Reactions were quenched by the addition of SDS loading buffer, and proteins were resolved by 16% SDS-PAGE and stained with Coomassie blue. The position of the protein markers lysozyme (14 kDa) and phosphorylase b (97 kDa) are indicated, but the protein bands are not shown.

To test this hypothesis further, we then determined if FusC is able to cleave human ferredoxin 1 and 2, which, despite sharing limited sequence identity with *Arabidopsis* ferredoxin, possess a common core fold with plant ferredoxins and a [2Fe-2S] iron-sulfur cluster. Similarly, no activity against these distantly related ferredoxins was observed, indicating that FusC has a highly targeted proteolytic activity (Fig. 1*B*).

Targeted Cleavage of Ferredoxin Results in Iron Release and Growth Under Iron-Limiting Conditions. To further probe plant ferredoxin cleavage by FusC, we attempted to map cleavage sites of Fer_{Ara}. Using SDS-PAGE with high percentage gels enabled us to identify two resolvable bands corresponding to cleavage products of Fer_{Ara} (Fig. 2*A*). These cleavage products were not further degraded with time and were stable as the concentration of FusC increased by 10-fold to 10 μM (*SI Appendix*, Fig. S2), indicating that proteolysis of Fer_{Ara} by FusC occurs specifically at a small number of sites. N-terminal sequencing of these cleavage products gave a sequence of LDDEQ for the upper band, with no sequence obtained for the lower band. The N-terminal sequence of this fragment indicates cleavage of Fer_{Ara} between F64 and L65.

Further analysis by MALDI-TOF mass spectrometry of Fer_{Ara} cleavage products directly from solution after incubation with FusC, indicated the presence of three peptides corresponding to cleavage products of Fer_{Ara} (Fig. 2*B*). Consistent with the results from N-terminal sequencing, the low-intensity peak corresponding to a peptide with an observed mass of 4,693.0 Da is close to the expected mass (4,690.2 Da) of the C-terminal fragment from cleavage of Fer_{Ara} before the identified LDDEQ sequence between F64 and L65. The observed peptide mass of 3,152.6

MICROBIOLOGY

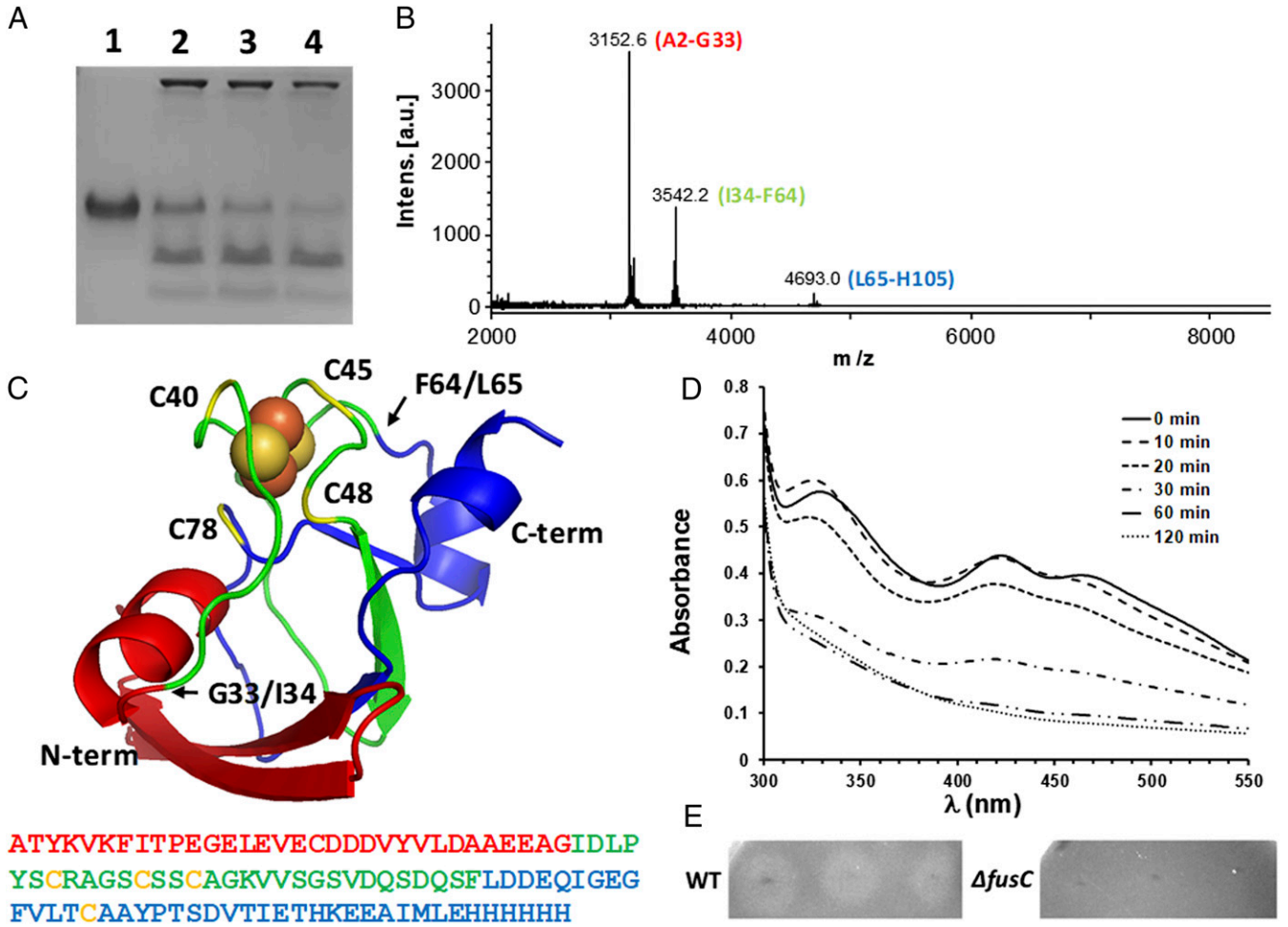

Fig. 2. Targeted cleavage of ferredoxin results in iron release. (*A*) Limited proteolysis of Fer_{Ara} by FusC. Purified His-tagged FusC (1 μM) was incubated with Fer_{Ara} (100 μM) at room temperature in 50 mM Tris·HCl and 50 mM NaCl, pH 7.5. Reactions were quenched by the addition of SDS loading buffer, and proteins were resolved by 18% SDS-PAGE and stained with Coomassie blue. Lane 1: Fer_{Ara} alone, $t = 0$ min. Lanes 2, 3 and 4: Fer_{Ara} + FusC incubated for 30, 60, and 90 min, respectively. (*B*) FusC cleaves two peptide bonds in Fer_{Ara}. Three peptides, corresponding to N-terminal (A2–G33), central (I34–F64) and C-terminal (L65–H105) regions of Fer_{Ara} were detected by MALDI-TOF MS. (*C*) Structure of *Arabidopsis* ferredoxin (PDB ID code 4ZHO) (22) highlighting cleavage sites and resulting N-terminal (red), central (green), and C-terminal (blue) peptides. The iron-coordinating cysteine residues C40, C45, C48, and C78 are highlighted in yellow. The corresponding sequence is shown below. (*D*) Fer_{Ara} cleavage leads to loss of the [2Fe-2S] cluster. Shown are absorption spectra of Fer_{Ara} (100 μM) on incubation with FusC (1 μM) for 0–120 min in 50 mM Tris·HCl and 50 mM NaCl, pH 7.5. (*E*) To test growth enhancement on solid media, purified Fer_{Ara} at 3.0, 1.0, and 0.33 mg/mL (left to right) was spotted (5 μL) onto a growing lawn of *P. carotovorum* LMG 2410 or LMG 2410 Δ*fusC* in the presence of 600 μM 2,2′-bipyridine. Plates were incubated for 24 h at 30 °C. The growth enhancement in WT but not in Δ*fusC* cells indicates that ferredoxin-enhanced growth is FusC-dependent.

corresponds closely to the expected mass (3,153.4) of the central region of Fer_{Ara} from I34 to F64 and the observed peptide mass of 3,542.2 is close to expected mass of the N-terminal region of Fer_{Ara} (A2–G33) plus the mass of a sodium ion (3,541.6). We suspect that the sodium adduct is observed for this protein due to the extreme negative charge of the 32-residue peptide, which contains a total of 10 aspartic acid and glutamic acid residues. No peptides were observed on analysis after incubation of FusC or Fer_{Ara} alone by MALDI-TOF mass spectrometry (*SI Appendix*, Fig. S3).

These data indicate that Fer_{Ara} contains two FusC cleavage sites between G33/I34 and F64/L65. In plant ferredoxins, coordination of the [2Fe-2S] cluster is mediated by four cysteine residues arranged into a conserved CX_4CXXCX_nC motif with three N-terminal cysteine residues present on an extruded loop that lies between the first α-helix and third β-stand in the ferredoxin structure (29) (Fig. 2*C*). In Fer_{Ara} [Protein Data Bank (PDB) ID code 47HO] (22), C40, C45, and C48 are present in the extruded loop, with C78 being the final coordinating cysteine. Interestingly, the G33/I34 cleavage site is located at the N terminus of the [2Fe-2S]-coordinating loop with the second F64/L65 site cleaving between the third and fourth [2Fe-2S]-coordinating cysteines (Fig. 2*C*). This suggests that cleavage at these sites will likely cause destabilization of the [2Fe-2S]-coordinating region of Fer_{Ara}.

To test this hypothesis, we incubated Fer_{Ara} with FusC and monitored the change in absorbance from 300 to 500 nm over time. Similar to other plant ferredoxins in their oxidized form, and due to coordination of the [2Fe-2S] cluster, the UV-vis spectrum of Fer_{Ara} displays distinct maxima at 330 nm, 423 nm, and 466 nm (30, 31). On incubation of Fer_{Ara} with FusC, we observed a time-dependent loss of absorption between 300 and 500 nm, and after 60 min, the complete disappearance of maxima at 330 nm, 423 nm, and 466 nm (Fig. 2*D*). On incubation of Fer_{Ara} alone, no change in the absorbance spectrum was observed, showing that the protein is stable in the absence of FusC (*SI Appendix*, Fig. S4). These data show that FusC-mediated cleavage of Fer_{Ara} leads to release of the [2Fe-2S] cluster.

FusC-mediated loss of the Fer_{Ara} [2Fe-2S] cluster suggests a role for FusC in the acquisition of iron by *Pectobacterium* spp. from plant ferredoxins, as we reported previously (19). To test this, we monitored growth enhancement of *P. carotovorum* LMG

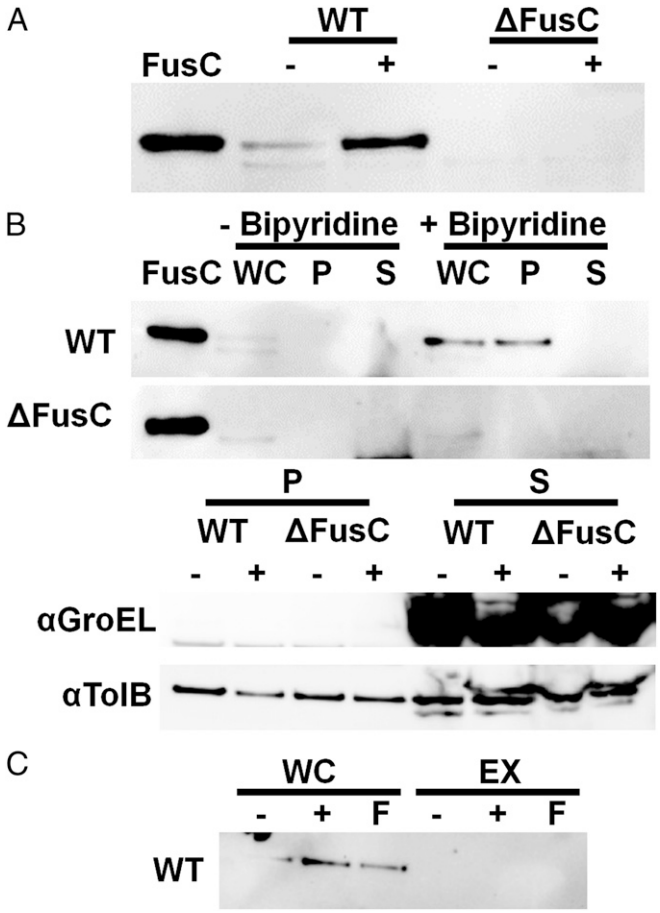

Fig. 3. FusC is an iron-regulated periplasmic protein. (*A*) FusC production is up-regulated under iron-limiting conditions. Whole-cell extracts of wild-type LMG2410 (WT) and LMG2410 Δ*fusC* (ΔFusC) from cells grown in the absence (–) or presence (+) of 200 μM bipyridine were subjected to immunoblotting with αFusC antibodies. Purified FusC was run in the left lane as a marker. (*B*) FusC is a periplasmic protein. (*Top*) Wild-type LMG2410 (WT) and LMG2410 Δ*fusC* (ΔFusC) cells grown in the absence (–) or presence (+) of 200 μM 2,2′ bipyridine were fractionated, and whole-cell (WC), periplasmic (P), and spheroplast fractions were immunoblotted using αFusC antibodies. Purified FusC was run in the left lane as a marker. (*Bottom*) Periplasmic and spheroplast fractions were also subjected to αGroEL immunoblotting to determine the level of spheroplast leakage. GroEL was not identified in the periplasmic fraction. αTolB antibodies were used as a marker of periplasmic proteins, although, as previously described in *E. coli*, TolB is also associated with the cytoplasmic membrane and therefore with spheroplasts, presumably due to its interaction with the inner membrane TolAQR complex (36). (*C*) FusC is not exported to the extracellular media. Whole-cell and precipitated proteins from the supernatant (EX) from LMG2410 (WT) cells grown in the absence (–) or presence (+) of 200 μM bipyridine or in the presence of 200 μM bipyridine and 1 μM Fer_{Ara} (F) were subjected to immunoblotting with αFusC antibodies. No FusC was detected in the extracellular medium.

2410 and an isogenic Δ*fusC* strain after the addition of Fer_{Ara} on solid media under iron-limiting conditions due to the presence of the iron chelator 2,2′-bipyridine (bipyridine). Zones of growth enhancement due to the addition of purified Fer_{Ara} were observed for wild-type LMG 2410, but not for LMG 2410 Δ*fusC*, indicating that iron acquisition by *Pectobacterium* spp. from plant ferredoxin requires FusC-mediated cleavage and iron release (Fig. 2*E*). Enhancement of growth on the addition of Fer_{Ara} in liquid media was also observed to a greater extent for wild-type *P. carotovorum* LMG 2410 relative to the Δ*fusC* strain. For wild-type LMG 2410, a 52% increase (relative to no Fer_{Ara} addition) in OD_{600} after 5 h of growth in the presence of 0.2 μM Fer_{Ara} was observed, compared with an 11% increase for the Δ*fusC* strain (*SI Appendix*, Fig. S5).

Ferredoxin Is Cleaved by FusC After Uptake to the Periplasm. To determine whether ferredoxin cleavage occurs in the periplasm or on the external cell surface, we attempted to determine the cellular location of FusC. FusC is synthesized as a 924-aa polypeptide with a predicted 25-aa signal sequence (SignalP 4.1) (32) that is cleaved on Sec-mediated export to the periplasm, indicating a potential periplasmic location for the mature 101-kDa protein. In an attempt to confirm the cellular location of FusC, we raised antibodies to peptides from the FusC sequence and used these to probe fractionated cell extracts and precipitated proteins from *P. carotovorum* LMG 2410, as well as the isogenic Δ*fusC* strain by immunoblotting. Initial experiments with whole-cell extracts indicated that FusC production is strongly regulated by iron availability, with FusC production up-regulated under conditions of iron limitation due to the presence of the iron chelator bipyridine (Fig. 3*A*). Probing of fractionated cell extracts showed that FusC could be detected in the periplasmic extract, but not in the cytoplasmic contents or among proteins exported to the extracellular media (Fig. 3 *B* and *C*). Thus, FusC is an iron-regulated periplasmic protein.

In many bacteria, iron homeostasis is controlled by the ferric uptake regulator protein (Fur), a transcriptional regulator that binds to the Fur box, a conserved DNA sequence located within the promoter regions of iron-regulated genes. In *P. carotovorum*, *fur* regulates traits important to host–pathogen interactions, and its deletion results in increased siderophore production (33). The sequence of the *P. carotovorum* Fur box is not well characterized, however.

Since FusC has a periplasmic location, we reasoned that a Δ*fusC* strain, which could not proteolytically process ferredoxin, would accumulate Fer_{Ara} in the periplasm. To test this, we grew wild-type and Δ*fusC P. carotovorum* LMG 2410 in the presence of Fer_{Ara}, bipyridine, or both Fer_{Ara} and bipyridine until an OD_{600} ≈1 and tested for the presence of Fer_{Ara} in the whole-cell and periplasmic fractions, as well as in the growth media after capture with nickel-affinity beads. In the Δ*fusC* strain grown in the presence of ferredoxin or with ferredoxin and bipyridine, we detected Fer_{Ara} in both the whole-cell and periplasmic fractions but not in the media, indicating that the Δ*fusC* strain is able to translocate Fer_{Ara} into the periplasm but cannot process it further. For the wild-type strain, we detected a small amount of Fer_{Ara} in the media in the presence of ferredoxin alone but did not detect Fer_{Ara} in the whole-cell or periplasmic fractions in any conditions, indicating that *Pectobacterium* with an intact Fus system can efficiently translocate and process ferredoxin (Fig. 4*A*).

To further investigate the kinetics of Fer_{Ara} uptake, we grew *P. carotovorum* LMG 2410 Δ*fusC* in the presence of Fer_{Ara} and bipyridine and tested for the presence of Fer_{Ara} in whole-cell extracts at 15, 45 and 120 min. After 15 min, Fer_{Ara} was not detected in whole-cell extracts but was detected in increasing amounts at 45 and 120 min, respectively (Fig. 4*B*). Fractionation of cells and measurement of ferredoxin levels in spheroplasts and periplasmic extracts from cells harvested at these time points, along with levels in the growth media, show that time-dependent accumulation of Fer_{Ara} in the periplasm is accompanied by a concomitant decrease in Fer_{Ara} levels in the media to very low levels at 120 min (Fig. 4*C* and *SI Appendix*, Fig. S6). Plasmid-based complementation showed that reintroduction of *fusC* into *P. carotovorum* LMG 2410 Δ*fusC* was able to completely reverse periplasmic ferredoxin accumulation on isopropyl-B-D-thiogalactopyranoside (IPTG)-mediated induction of FusC production (Fig. 4*D*).

Discussion

In this work, we build on our previous identification of the ferredoxin receptor FusA and show that the periplasmic protease FusC has highly targeted activity against plant ferredoxin, and that iron acquisition by *Pectobacterium* spp. from ferredoxin is FusC-dependent. Thus, in our current model of Fus-mediated iron acquisition (Fig. 5), the substrate is bound at the cell surface by the

MICROBIOLOGY

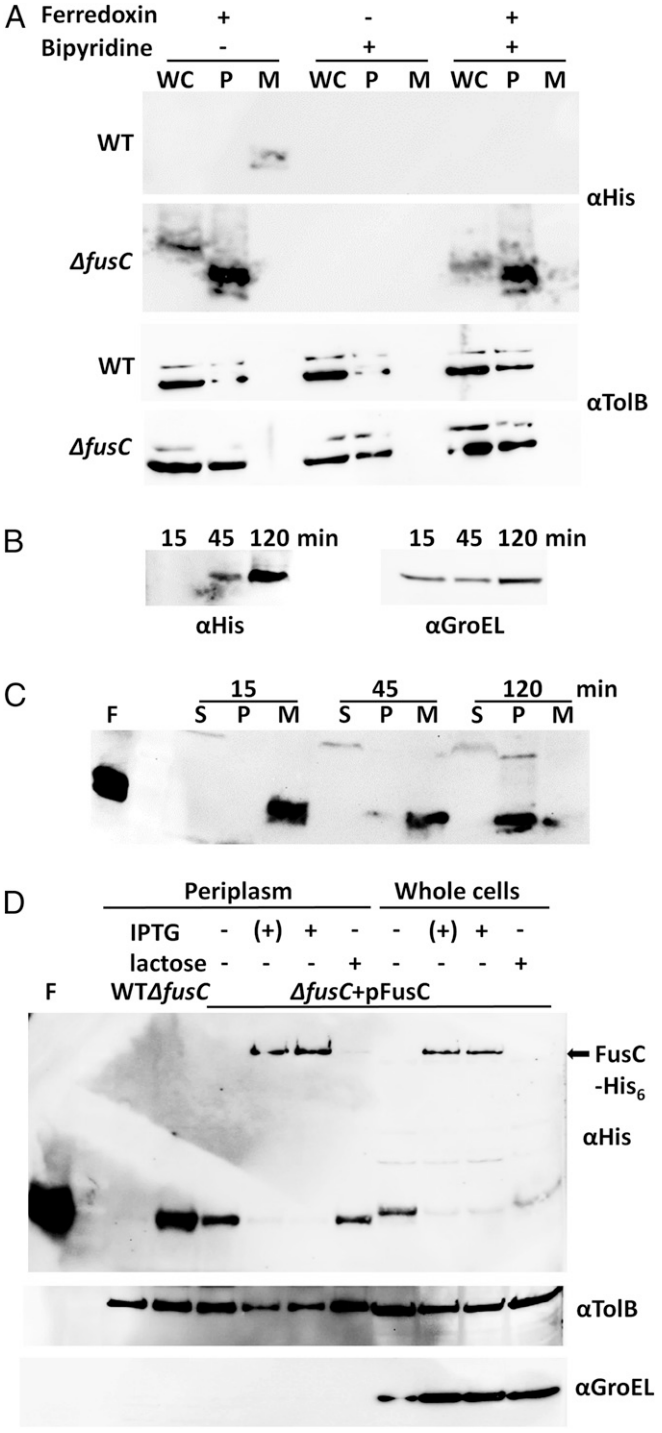

Fig. 4. Ferredoxin is translocated to the periplasm for FusC-dependent processing. (*A*) Internalization assay showing the accumulation of ferredoxin in *P. carotovorum* LMG2410 Δ*fusC*, but not in WT cells. The cells were cultured in M9 media in the presence or absence of 1 μM ferredoxin or 100 μM 2,2′-bipyridine until OD_{600} ≈1 and then subjected to fractionation, whole cells (WC) and periplasmic fraction (P). M, elution from nickel beads after incubation with filtered growth media. (*Top*) His-tagged Fer_{Ara} is detected by the αHis antibody showing that Fer_{Ara} can be detected in whole-cell and periplasmic fractions in the Δ*fusC* strain, but not in the WT strain due to proteolytic processing by FusC. Preliminary experiments showed that Fer_{Ara} migrates anomalously in whole-cell fractions due to the presence of BugBuster. (*Bottom*) Blots reprobed with αTolB antibodies. (*B*) Time course of ferredoxin internalization in *P. carotovorum* LMG2410 Δ*fusC*. Fer_{Ara} content in the whole cells (*Left*) together with the GroEL loading control (*Right*). (*C*) Fractionation of cells from the time course in *B*; spheroplast (S), periplasm (P), and media (M) fractions at each time point are shown. F, purified Fer_{Ara} control. Fer_{Ara} levels decreased in the media over the course of the experiment and progressively accumulated in the periplasm. (*D*) Plasmid based complementation of *P. carotovorum* LMG2410 Δ*fusC* with pFusC restores ferredoxin processing. WT, Δ*fusC*, and recomplemented Δ*fusC*+pFusC cells were cultured in LB media until OD_{600} ≈0.4, after which FusC expression in two of the Δ*fusC*+pFusC cultures was induced by the addition of 1 mM IPTG or 1% lactose. One Δ*fusC*+pFusC culture labeled (+) contained 0.2 mM IPTG added at the start. At 30 min postinduction, 1 μM ferredoxin and 200 μM 2,2′-bipyridine were added to each culture, and after 2 h, the cells were fractionated. Purified Fer_{Ara} was run in the lane marked F. TolB and GroEL loading controls probed with αTolB and αGroEL antibodies, respectively, are shown at the bottom.

TBDR FusA and is translocated into the periplasm in a process presumably involving FusB, a TonB homolog that is conserved in the Fus operon of *Pectobacterium* spp. However, the exact role of FusB remains to be proven, and it can be envisaged that FusB acts in a similar manner to TonB through interaction with a TonB-box of the TBDR to mediate extraction of the FusA plug domain. Alternatively, if endogenous TonB is able to fulfill this role, then FusB may mediate the energy-dependent translocation of ferredoxin into the cell by direct contact with the substrate subsequent to extraction of the plug domain by TonB. On translocation into the periplasm, ferredoxin is then cleaved by FusC, triggering release of the [2Fe-2S] cluster, which we hypothesize is transported to the cytoplasm in a process that may be mediated by the putative ABC transporter encoded by *fusD*.

As we have described previously, homologs of the *fus* operon that minimally encode a TBDR and an M16 protease are found in the genomes of a range of pathogenic Gram-negative bacteria, including *E. coli* and members of the genera *Neisseria* and *Yersinia* and the Pasteurellaceae (22). Although in these cases the substrate has not been identified, the presence of a genes encoding a large (approximate 100 kDa) TBDR (TBDRs that bind siderophores are typically much smaller at 70–80 kDa) and a periplasmic M16 protease suggest a protein substrate, indicating that uptake and cleavage of proteins for nutrient acquisition may be widespread in bacteria.

The existence of dedicated and highly specific protein uptake systems in Gram-negative bacteria suggests that receptor-mediated protein uptake in mitochondria and plastids might not have evolved independently of their bacterial ancestors, although whether this indeed is the case remains to be determined. However, it is interesting to note that the processing of proteins imported into these organelles is mediated in part by M16 protease family members, such as the mitochondrial processing peptidase and presequence protease that cleave and degrade signal peptides of imported mitochondrial proteins (24, 25).

Materials and Methods

Bacterial Strains and Media. *E. coli* was grown in LB broth or plated on LB agar in the presence of ampicillin (100 μg mL^{-1}). DH5α and BL21 (DE3) strains were used as host strains for cloning and for IPTG-induced protein expression, respectively. *E. coli* strains were grown at 37 °C, and *P. carotovorum* strains were grown in LB broth or plated on LB agar at 30 °C with the addition of the iron chelator 2,2′-bipyridine where specified.

Protein Purification. FusC was expressed in *E. coli* BL21 (DE3) carrying the plasmid pFusC, which encodes FusC from *P. atrosepticum* SCRI1043 with an additional LEHHHHHH sequence for purification by nickel-affinity chromatography at the C terminus. More details are provided in *SI Appendix, Materials and Methods*. *Arabidopsis* ferredoxin (Fer_{Ara}) was purified as described previously (22), and human ferredoxin 1 (FerH1) and human ferredoxin 2 (FerH2) were purified with the same method from BL21 (DE3) cells harboring the plasmids pHFdx1and pHFdx2, respectively. E3RNase, E3RNase Y64A Im3, and E3RNase Y64A Im6 were purified as described previously (27, 28).

Proteolytic Activity and Iron Release. Purified FusC and potential substrate proteins were incubated in 50 mM Tris·HCl and 50 mM NaCl, pH 7.5, at room temperature at the specified concentrations. Samples were removed at the

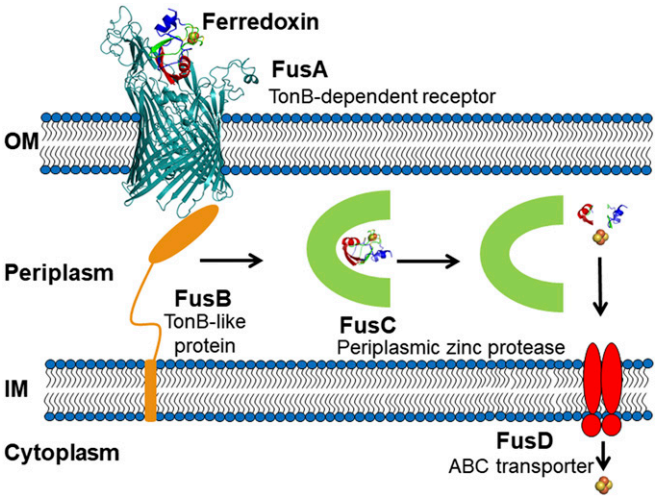

Fig. 5. Schematic representation of Fus-dependent import and processing of ferredoxin. Ferredoxin is imported via the TBDR FusA (22) presumably mediated by the TonB homolog FusB, which may play a conventional TonB-like role in removal of the plug domain from the lumen of FusA, or may directly contact the substrate. On transport to the periplasm, FusC cleaves ferredoxin, and we hypothesize this leads to the release of the [2Fe-2S] cluster, which may be transported to the cytoplasm by the putative ABC transporter FusD. The exact form of iron present in the periplasm on release from ferredoxin remains to be determined, however.

indicated time points, and the reaction was quenched by the addition of SDS loading buffer. Samples were heated to 95 °C for 2 min and then analyzed by SDS-PAGE. MALDI-TOF mass spectrometry was performed on FusC, Fer_{Ara}, and FusC + Fer_{Ara} after incubation at room temperature for 1 h in 50 mM Tris·HCl and 200 mM NaCl, pH 7.5, and quenching with 1 mM EDTA with Fer_{Ara} at 10 μM and FusC at 1 μM. Details the MALDI-TOF analysis are provided in *SI Appendix, Materials and Methods*.

To follow the release of iron from *Arabidopsis* ferredoxin resulting from the proteolytic activity of FusC, we measured the absorbance spectra of Fer_{Ara} (100 μM) alone or Fer_{Ara} (100 μM) mixed with FusC (1 μM) from 0 to 120 min. Experiments were performed in 50 mM Tris·HCl and 50 mM NaCl, pH 7.5, and spectra were recorded on a Shimadzu UV-1700 spectrophotometer using 1-cm path length quartz cuvettes.

Creation of *P. carotovorum* LMG2410 ΔfusC. The sequence of the *P. carotovorum* LMG2410 FusC gene was determined by amplifying and sequencing PCR products using a forward primer (5′-CGA GTT TCA ATA CTG CCA TTG TC-3′) that anneals within the 3′ end of the FusA gene (sequence data available) and a reverse primer (5′-CACTCTTTCACCTCTTG-3′) based on sequence downstream of FusC gene that is conserved across different strains of *Pectobacterium* spp. The FusC gene was deleted using the lambda red protocol (34) as described in *SI Appendix, Materials and Methods*.

Growth Enhancement Assays. Enhancement of growth on solid media was determined using the soft agar overlay method (19, 35), as described along with the method used for growth enhancement in liquid culture in *SI Appendix, Materials and Methods*.

FusC Localization. FusC was localized by cell fractionation and immunoblotting using an αFusC antibody, raised to two peptides (RVQAIRHDSRYSR and LARQKANDDQSV) in rabbits and subsequently affinity-purified (Eurogentec). Cell fractionation was achieved by the formation of spheroplasts and isolation of the periplasmic fraction. Whole-cell extracts were obtained using BugBuster Protein Extraction Reagent (Merck). To determine if FusC is exported into the extracellular medium, protein in the supernatant was precipitated with trichloroacetic acid. More information is provided in *SI Appendix, Materials and Methods*.

Ferredoxin Internalization. The ferredoxin internalization assays are described in detail in *SI Appendix, Materials and Methods*.

ACKNOWLEDGMENTS. This work was funded by the Biotechnology and Biological Sciences Research Council (Grant BB/L02022X/1).

1. Palmer LD, Skaar EP (2016) Transition metals and virulence in bacteria. *Annu Rev Genet* 50:67–91.
2. Cornelissen CN (2017) Subversion of nutritional immunity by the pathogenic *Neisseriae*. *Pathog Dis* 76:ftx112.
3. Chu BC, et al. (2010) Siderophore uptake in bacteria and the battle for iron with the host: A bird's eye view. *Biometals* 23:601–611.
4. Noinaj N, Buchanan SK, Cornelissen CN (2012) The transferrin-iron import system from pathogenic *Neisseria* species. *Mol Microbiol* 86:246–257.
5. Noinaj N, Guillier M, Barnard TJ, Buchanan SK (2010) TonB-dependent transporters: Regulation, structure, and function. *Annu Rev Microbiol* 64:43–60.
6. Celia H, et al. (2016) Structural insight into the role of the Ton complex in energy transduction. *Nature* 538:60–65.
7. Hickman SJ, Cooper REM, Bellucci L, Paci E, Brockwell DJ (2017) Gating of TonB-dependent transporters by substrate-specific forced remodelling. *Nat Commun* 8: 14804.
8. Pawelek PD, et al. (2006) Structure of TonB in complex with FhuA, *E. coli* outer membrane receptor. *Science* 312:1399–1402.
9. Ferguson AD, et al. (2002) Structural basis of gating by the outer membrane transporter FecA. *Science* 295:1715–1719.
10. Howard SP, Herrmann C, Stratilo CW, Braun V (2001) In vivo synthesis of the periplasmic domain of TonB inhibits transport through the FecA and FhuA iron siderophore transporters of *Escherichia coli*. *J Bacteriol* 183:5885–5895.
11. Noinaj N, et al. (2012) Structural basis for iron piracy by pathogenic *Neisseria*. *Nature* 483:53–58.
12. Kleanthous C (2010) Swimming against the tide: Progress and challenges in our understanding of colicin translocation. *Nat Rev Microbiol* 8:843–848.
13. Housden NG, Kleanthous C (2012) Colicin translocation across the *Escherichia coli* outer membrane. *Biochem Soc Trans* 40:1475–1479.
14. Jakes KS, Cramer WA (2012) Border crossings: Colicins and transporters. *Annu Rev Genet* 46:209–231.
15. Killmann H, Braun V (1994) Energy-dependent receptor activities of *Escherichia coli* K-12: Mutated TonB proteins alter FhuA receptor activities to phages T5, T1, phi 80 and to colicin M. *FEMS Microbiol Lett* 119:71–76.
16. Denayer S, Matthijs S, Cornelis P (2007) Pyocin S2 (Sa) kills *Pseudomonas aeruginosa* strains via the FpvA type I ferripyoverdine receptor. *J Bacteriol* 189:7663–7668.
17. Kurisu G, et al. (2003) The structure of BtuB with bound colicin E3 R-domain implies a translocon. *Nat Struct Biol* 10:948–954.
18. White P, et al. (2017) Exploitation of an iron transporter for bacterial protein antibiotic import. *Proc Natl Acad Sci USA* 114:12051–12056.
19. Grinter R, Milner J, Walker D (2012) Ferredoxin containing bacteriocins suggest a novel mechanism of iron uptake in *Pectobacterium* spp. *PLoS One* 7:e33033.
20. Grinter R, Milner J, Walker D (2013) Beware of proteins bearing gifts: Protein antibiotics that use iron as a Trojan horse. *FEMS Microbiol Lett* 338:1–9.
21. Grinter R, et al. (2014) Structure of the atypical bacteriocin pectocin M2 implies a novel mechanism of protein uptake. *Mol Microbiol* 93:234–246.
22. Grinter R, et al. (2016) Structure of the bacterial plant-ferredoxin receptor FusA. *Nat Commun* 7:13308.
23. Aleshin AE, et al. (2009) Crystal and solution structures of a prokaryotic M16B peptidase: An open and shut case. *Structure* 17:1465–1475.
24. King JV, et al. (2014) Molecular basis of substrate recognition and degradation by human presequence protease. *Structure* 22:996–1007.
25. Teixeira PF, Glaser E (2013) Processing peptidases in mitochondria and chloroplasts. *Biochim Biophys Acta* 1833:360–370.
26. Hooper NM (1994) Families of zinc metalloproteases. *FEBS Lett* 354:1–6.
27. Papadakos G, et al. (2015) Consequences of inducing intrinsic disorder in a high-affinity protein-protein interaction. *J Am Chem Soc* 137:5252–5255.
28. Walker D, Moore GR, James R, Kleanthous C (2003) Thermodynamic consequences of bipartite immunity protein binding to the ribosomal ribonuclease colicin E3. *Biochemistry* 42:4161–4171.
29. Bertini I, Sigel A, Sigel H (2001) *Handbook on Metalloproteins* (Marcel Dekker, New York).
30. Hall DO, Cammack R, Rao KK (1973) The plant ferredoxins and their relationship to the evolution of ferredoxins from primitive life. *Pure Appl Chem* 34:553–578.
31. Mayhew SG, Petering D, Palmer G, Foust GP (1969) Spectrophotometric titration of ferredoxins and chromatium high-potential iron protein with sodium dithionite. *J Biol Chem* 244:2830–2834.
32. Petersen TN, Brunak S, von Heijne G, Nielsen H (2011) SignalP 4.0: Discriminating signal peptides from transmembrane regions. *Nat Methods* 8:785–786.
33. Tanui CK, Shyntum DY, Priem SL, Theron J, Moleleki LN (2017) Influence of the ferric uptake regulator (Fur) protein on pathogenicity in *Pectobacterium carotovorum* subsp. *brasiliense*. *PLoS One* 12:e0177647.
34. Datsenko KA, Wanner BL (2000) One-step inactivation of chromosomal genes in *Escherichia coli* K-12 using PCR products. *Proc Natl Acad Sci USA* 97:6640–6645.
35. Fyfe JA, Harris G, Govan JR (1984) Revised pyocin typing method for *Pseudomonas aeruginosa*. *J Clin Microbiol* 20:47–50.
36. Isnard M, Rigal A, Lazzaroni JC, Lazdunski C, Lloubes R (1994) Maturation and localization of the TolB protein required for colicin import. *J Bacteriol* 176:6392–6396.